Electronic Supplementary Material (ESI) for Integrative Biology

Supplementary Online Material for

The plant cell uses carbon nanotubes to build tracheary elements

Maged F. Serag,*[a] Noritada Kaji,[a,b] Manabu Tokeshi, Alberto Bianco,[c] and Yoshinobu Baba[a,b,d]

[a] *Department of Applied Chemistry, Graduate School of Engineering, Nagoya University, Nagoya, JAPAN. Fax: +81-52-789-4666; Tel: +81-52-789-3560; E-mail: m.serag@nanobio-nagoya-u.ac.jp*
[b] *FIRST Research Centre for Innovative Nanodevices, Nagoya University, JAPAN.*
[c] *Centre National de la Recherche Scientifique, Institut de Biologie Moléculaire et Cellulaire, UPR 9021 Immunologie et Chimie Thérapeutiques, Strasbourg, FRANCE.*
[d] *National Institute of Advanced Industrial Science and Technology (AIST), Takamatsu, JAPAN.*

This PDF file includes:

Supporting Online Materials

Table of contents

1. Materials and methods

Carbon nanotubes covalent immobilization on polymethyl methacrylate (PMMA) surface

i) Basic concept:

Biocatalysis in non-aqueous media is becoming increasingly important in organic synthesis. Lipases are the most used enzymes especially in trans-esterification reactions. Lipases also catalyze the formation of amides from non-activated esters [*V. Gotor. Lipases and (R)-oxynitrilases: useful tools in organic synthesis. Journal of Biotechnology,* ***96****, 35 (2002)*]. Utilizing lipases chemical characteristics in organic solvents, we proposed a chemical reaction in which PMMA can be amidated with diethylene triamine (DETA) in presence of *Candida Cylindracea* lipase (CCL). The free amino group of the formed amide was then linked to carbon nanotubes via a carbodiimide reaction using EDC reagent (Fig. M1).

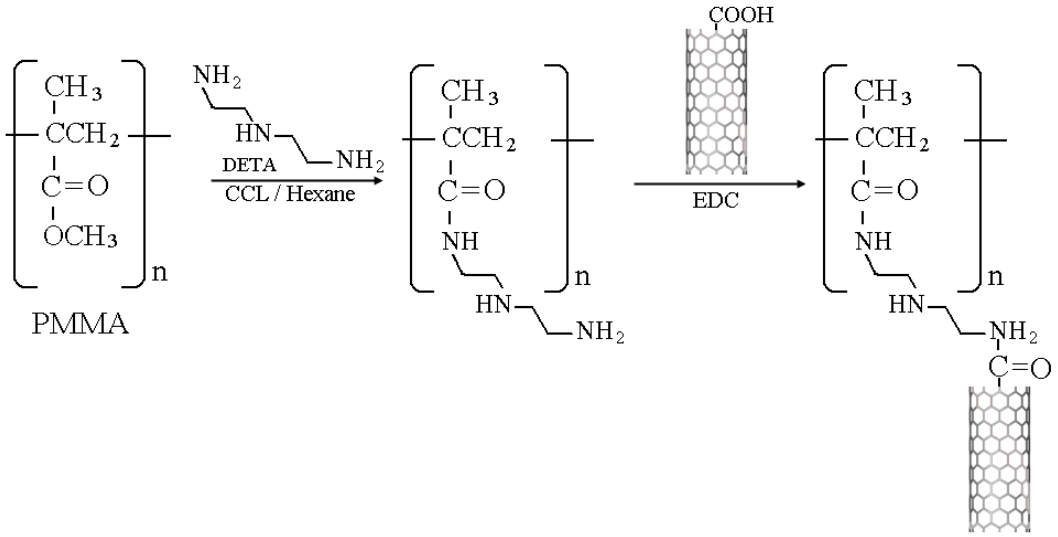

Figure M1. Scheme of the proposed steps for nanotube immobilization on PMMA surface.

ii) Experimental (All chemicals were purchased from Sigma (St. Louis, M.O., USA).

Lipase-Catalyzed amidation of PMMA. PMMA discs (3 mm diameter; Hitachi, Inc. Japan) were used for nanotubes immobilization. Discs were suspended in 10 mL anhydrous hexane. Three hundred mg of *Candida Cylindracea* lipase was added and the mixture was stirred magnetically. 20 µL of diethylenetriamine were added gradually with continuous stirring. The reaction mixture was incubated overnight at room temperature. Discs were vortexed in MES buffer and the supernatant was discarded. The buffer wash was repeated to remove excessive reagents.

Carbon nanotube functionalization via activated carboxylic groups. Twenty mg of CSCNTs were sonicated in 60% nitric acid for 30 min then refluxed at 120ºC overnight. The dispersion was washed repeatedly with water and filtered until pH ~ 7. The resulting oxidized CSCNT were then dried under vacuum overnight. One mg of carboxylated CSCNTs was dispersed in 2 mL pH 6 MES buffer and sonicated for 10 min. The homogeneous dispersion was then mixed with 1 mL of 400 mM EDC reagent and 100 mL NHSS and vortexed at room temperature for 15 min. The resulting mixture was centrifuged at 15 000 rpm for 5 min, and the supernatent was discarded. The buffer wash was repeated to remove excessive EDC and NHSS.

Carbon nanotube covalent immobilization on PMMA surface. PMMA discs with the adaptor DETA molecule were stirred magnetically in a dispersion of activated nanotubes in MES buffer for 12 h. Finally, PMMA discs were filtered, washed with fresh MES buffer and dried under vacuum.

iii) Method validation

Figure M2 shows FT-IR analysis of PMMA surface after reaction with DETA. The graph shows double peaks at 1698 cm^{-1} and 1722 cm^{-1} which are attributed to amide and ester carbonyls,

respectively. This confirmed successful modification of PMMA surface with DETA molecules to be suitable for CNTs immobilization. Figure M3 shows ESEM imaging of PMMA surface after nanotube immobilization (images were captured using FEI Quanta600 microscope). Long CSCNT were observed to overlay the surface, while short nanotubes were observed to stand in an upright position.

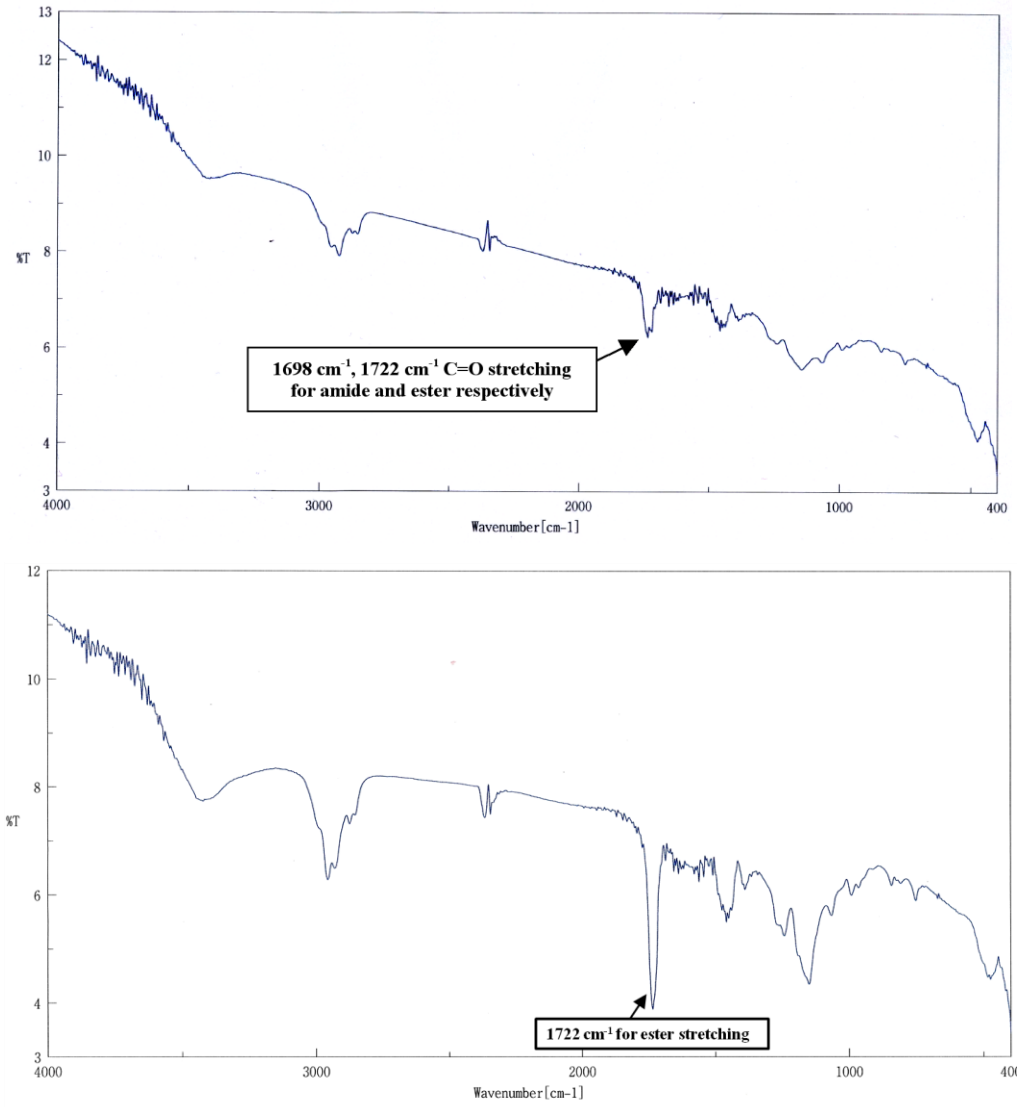

Figure M2. FT-IR of DETA-modified PMMA surface (top) and unmodified PMMA surface (bottom).

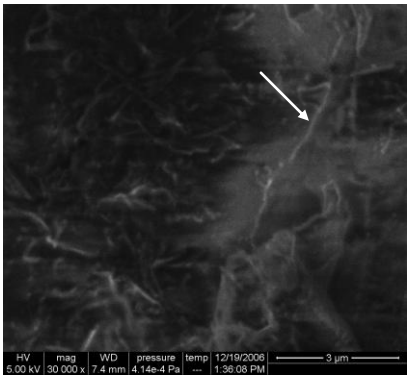

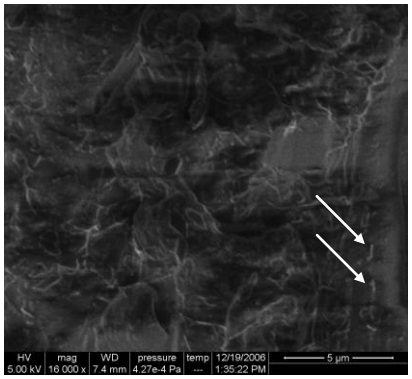

Figure M3. ESEM imaging of immobilized CSCNTs (arrows).

3. Supplementary Text

The multi-component structure of lignin makes its emission fluorescence spectrum to cover a relatively wide wavelength-scale ranging from 300-450 nm and peaking at 360 nm (such peak is achieved by using an excitation wavelength ranging from 240-320 nm [Albinsson, B., Shiming, L., Lundquist, K. & Stomberg, R. The origin of lignin fluorescence. *J. Mol. Struct.* **508**, 19-27 (1999)]. Since our target was to monitor CSCNTs inside the structure of lignin, we avoided lignin staining using fluorophores such as acridine-orange (Excitation wavelength; 500 nm), where we found that its strong fluorescence masks the fluorescence of individual nanotubes (Excitation wavelength; 515 nm). Initially, we optimized the detection conditions to avoid the fluorescence overlap of both CSCNTs and lignin components, where CSCNTs fluoresce at a longer excitation wavelength that is 515 nm. The next challenge was to deconvolute the fluorescence of lignin components through optimization and proper choice of different laser wavelengths and choice of proper ban-pass filters. Such deconvolution enabled us to detect the fluorescence shift of lignin components that entrap CSCNTs and to visualize individual CSCNTs in such components. Full description of the optimized detection conditions can be found in the methods section of the manuscript.

4. Supplementary Figures

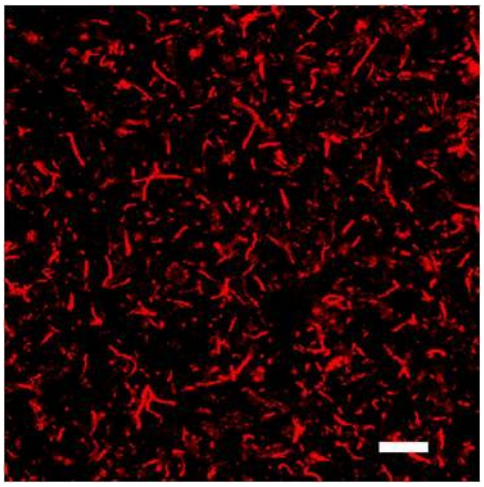

Supplementary Figure S1. Photoluminescence of CSCNTs. The image was recorded using the Qdot 525 band-passs filter while employing 515 nm laser. Scale bar: 10 µm.

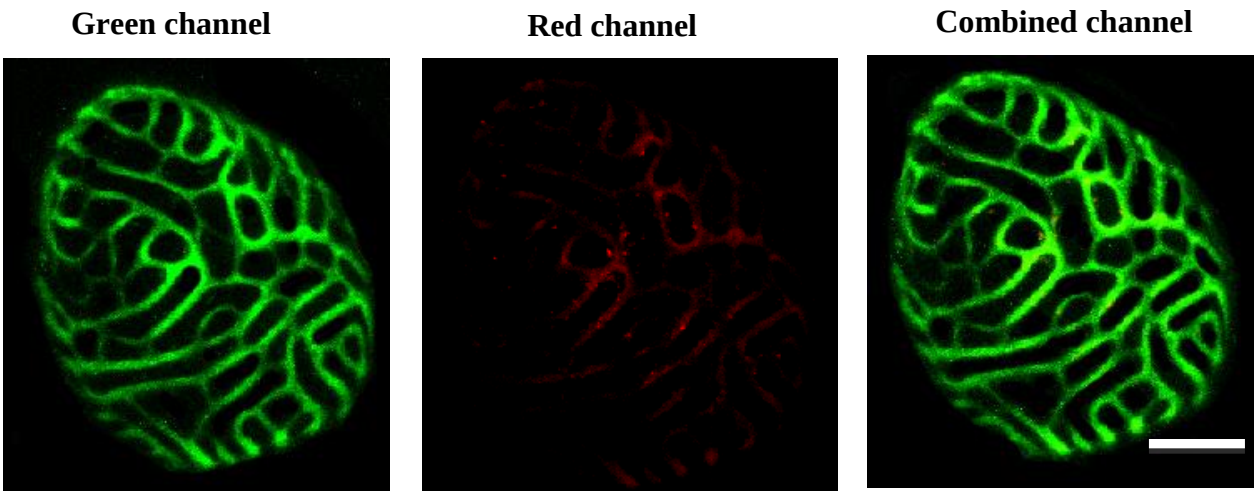

Supplementary Figure S2. 3D-reconstituted CLSM images of a normal tracheidal cell reconstituted from 80 optical single focal planes at 0.5 µm intervals. Fluorescence was recorded using the GFP-UV band-pass filter (Green), the Qdot 525 band-pass filter (red) and the combined channel. Scale bar: 10 µm.

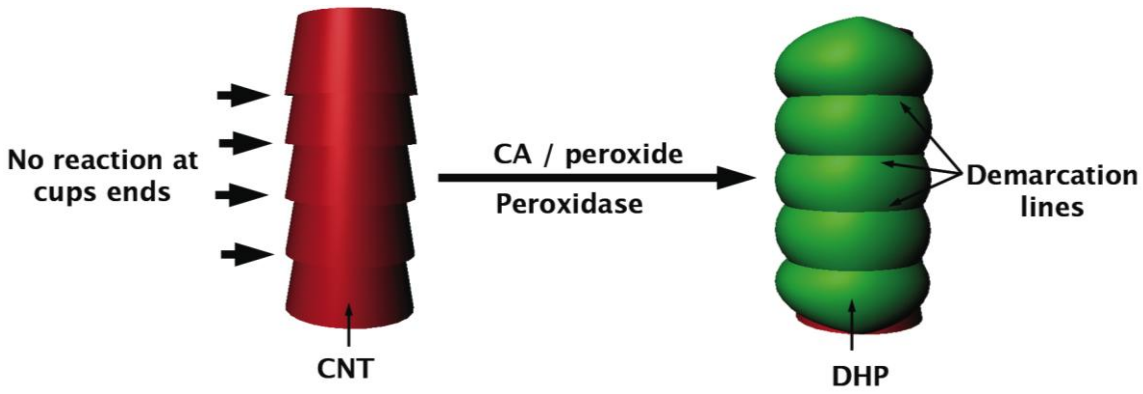

Supplementary Figure S3. 3D representation of DHP formation on CNT surface. Since CSCNTs are heavily functionalized at cups end, the upper and lower margins of the stacked cups do not participate in the polymerization reaction. This causes the appearance of demarcation lines in CNT-DHP macromolecules.

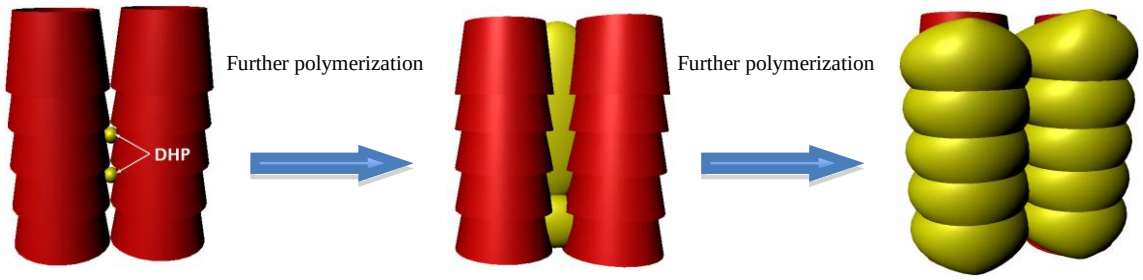

Supplementary Figure S4. We anticipated that the small CA molecules diffuse into the spaces between CSCNTs where they undergo polymerization into DHP. The gradual increase in DHP size held nanotubes apart from each other and results in mutual arrangement of nanotubes and DHP.

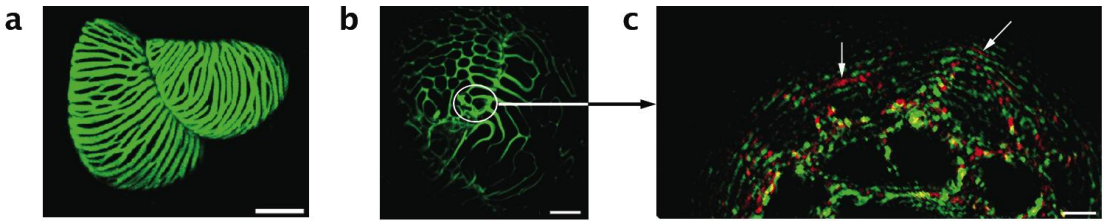

Supplementary Figure S5. Detection of Carbon nanotubes deposited between microtubules remnants. a. 3D-renderd CLSM images of normal tracheidal cells, reconstituted from 80 optical single focal planes at 0.5 µm intervals. Fluorescence was recorded in GFP-UV channel (Scale bar: 10 µm). **b.** 3D-reconstituted CLSM images of immature tracheidal cell, reconstituted from 80 optical single focal planes at 0.5 µm intervals. Fluorescence was recorded in GFP-UV channel (Scale bar: 8 µm). **c.** Single focal plane imaging of CSCNTs (red; arrows) between microtubules remnants (green). Fluorescence was recorded in the combined channel of Qdot 525 (red) and Oregon green (green). Scale bar: 2 µm.